

Evolution of the concept of Quark Matter: the Ianus face of the heavy ion collisions

J. Zimányi^a *

^aKFKI Research Institute for Nuclear and Particle Physics,
P.O. Box 49, H-1525 Budapest, Hungary

Since the beginning of the efforts to produce and understand quark matter large changes developed in the ideas of description of this matter. In the present paper we summarize some aspects of this development.

1. Evolution of ideas on quark matter

Since the beginning of the quest of quark matter deep changes have developed in our concept in understanding its properties. In Table 1 the ideas are collected, which dominated at the beginning of quark matter research. The present status of these ideas are also displayed. Although theoretical models supported the early concept, but the experimental data forced to change these speculations step by step. Thus the picture of a static, weakly interacting gaseous quark-gluon plasma was substituted by the more dynamic, strongly interacting fluid-like quark-gluon matter, where the ingredients gained an effective mass during the intense microscopical interactions.

Early times	Recent status
very high quark density;	not too high quark density;
vanishing coupling constant;	large effective coupling constant;
zero mass for quarks and gluons;	finite effective mass for quarks and gluons;
weakly interacting constituents;	strongly interacting constituents;
static, homogeneous gas;	dynamic, liquid-like system
very high temperature;	temperature near to critical;
vanishing sound velocity;	finite sound velocity;
long lifetime;	short lifetime;

Table 1

Concept of Quark Matter in the early times [1] and recently, considering the microstructure (upper part of the table) and the bulk properties (lower part of the table).

*The author thanks for the financial support of the OTKA grant T 49466. The author also thanks to the STAR collaboration for the permission of reproducing their result in Fig.7.

2. Time evolution of a heavy ion reaction

As soon as the static picture of quark gluon plasma was substituted by a dynamic scenario with short lifetime, the different pre-QGP and post-QGP stages became as important as the QGP state itself. As the dominance of a static plasma state has been lost, the dynamical steps and the intermediate phases ('matters') became the target of the theoretical investigations. Table 2 displays the emerged scenarios appearing in heavy ion collisions.

type of event	microscopic dynamics
color glass condensate (?)	gluon saturation [2]
evolution of plasma	expands and cools, undergoes through a set of phases [3]
prehadronization stage	quarks and antiquarks gather effective mass [4]
hadronization	quarks and antiquarks coalesce into hadrons [5]

Table 2

Time evolution of a heavy ion reaction.

In a heavy ion collision not a single sort, well defined type of matter is formed, but a set of different types of matter is created in the consecutive stages of the reaction.

3. Evolution of ideas on hadronization

In case of a quasi-static quark gluon plasma with long lifetime, there should be enough time for slow hadronization, which is driven by energy and momentum transformation at the macroscopical level. This leads to the application of thermodynamics. 15 years ago we were very much confident to expect a thermodynamical first order phase transition. As the time scale of the reaction became shorter, the idea of mixed phase transition appeared, handled with thermodynamical methods. However, as it turned out that the evolution of a heavy ion reaction is much faster, the hadronization ideas too had to be adjusted to this faster scenario. Finally, so fast hadronization processes must have been considered, that the macroscopical description was substituted by microscopical one and the slow thermodynamical transformation has been substituted by the fast process of coalescence of constituent quarks.

4. The coalescence models

The concept of quark coalescence has been evolved through different steps. At first the idea of quark number conservation appeared and became a very useful tool [5]. Then the linear vs. nonlinear coalescence descriptions were investigated [6]. Later on the description was improved and the direct momentum conservation at the microscopical level was considered in the coalescence processes [7, 8, 9]. Finally mass conservation has also been studied to produce light hadrons from heavy constituent quarks [10].

4.1. Coalescence hadronization with constituent quark number conservation

For the description of hadrons the constituent quark model was quite successful. In this approach the quarks are dressed, with mass of approximatively 300 MeV. The question arises, that at what stage of hadronization is this effective mass created? In the ALCOR model [5] it is assumed that this effective mass is created in the very last stage, in the prehadronization stage of the evolution of fireball.

The main assumptions of the ALCOR model:

- A) At the beginning of hadronization the quarks are dressed constituent quarks.
- B) These quarks coalesce to form the hadrons.
- C) The number of different quarks and antiquarks is conserved during hadronization.
- D) The effective mass of gluons is much higher than that of quarks near the critical temperature. Thus the gluon degree of freedom is neglected in this late period of the heavy ion reaction.
- E) The number of a given type of hadrons is proportional to the product of the numbers of different quarks from which the hadron consists:

$$N_{B,(ijk)} = C_{B,(ijk)} \cdot (b_i \cdot N_i) \cdot (b_j \cdot N_j) \cdot (b_k \cdot N_k) \quad (1)$$

where $N_{B,(ijk)}$ is the number of produced baryons from quark i, j, k , and the equation for quark number conservation in the hadronization $N_i^{Hadronmatter} = N_i^{QM} = N_i$ determines the b_i normalization coefficients.

With these assumptions one gets the relative numbers of particles in good agreement with experimental data, see Table 3.

	ALCOR model	STAR data	Ref.
h^-	280	280 ± 20	[11]
K^-/π^-	0.159	0.161 ± 0.002	[12]
K^+/K^-	1.091	1.092 ± 0.023	[13]
\bar{p}/p^+	0.66	0.71 ± 0.05	[14]
$\bar{\Lambda}/\Lambda$	0.72	0.71 ± 0.01	[13]
$\bar{\Xi}^+/\Xi^-$	0.80	0.83 ± 0.04	[13]
Ξ^-/h^-	0.0091	0.0077 ± 0.001	[15]
Φ/K^{*0}	0.42	0.49 ± 0.12	[16]

Table 3

Hadron production in Au+Au collision at $\sqrt{s} = 130$ AGeV from the ALCOR model and experimental data from the STAR Collaboration [11, 12, 13, 14, 15, 16].

4.2. The simple quark counting

Realizing [6] that the coalescence probabilities for a hadron and its antiparticle are the same: $C_h = C_{\bar{h}}$, very transparent relations can be obtained for the ratios of the different multiplicities:

$$\frac{\bar{\Lambda}}{\Lambda} = \mathbf{D} \cdot \frac{\bar{p}}{p} \quad \frac{\bar{\Xi}}{\Xi} = \mathbf{D} \cdot \frac{\bar{\Lambda}}{\Lambda} \quad \frac{\bar{\Omega}}{\Omega} = \mathbf{D} \cdot \frac{\bar{\Xi}}{\Xi} \quad \mathbf{D} = \frac{\mathbf{K}}{\bar{\mathbf{K}}} \quad (2)$$

These predictions agree again with the experimental data, see Table 4 and Figure 1.

Ratios	STAR	SPS
K^+/K^-	1.092 ± 0.023	1.76 ± 0.06
$\{\bar{\Lambda}/\Lambda\}/\{\bar{p}/p\}$	0.98 ± 0.09	2.07 ± 0.21
$\{\bar{\Xi}/\Xi\}/\{\bar{\Lambda}/\Lambda\}$	1.17 ± 0.11	1.78 ± 0.15
$\{\bar{\Omega}/\Omega\}/\{\bar{\Xi}/\Xi\}$	1.14 ± 0.21	1.42 ± 0.22

Table 4

Compilation of experimental particle ratios obtained at RHIC energy $\sqrt{s} = 130$ AGeV [13] and SPS energy 17.3 AGeV [17, 18, 19, 20].

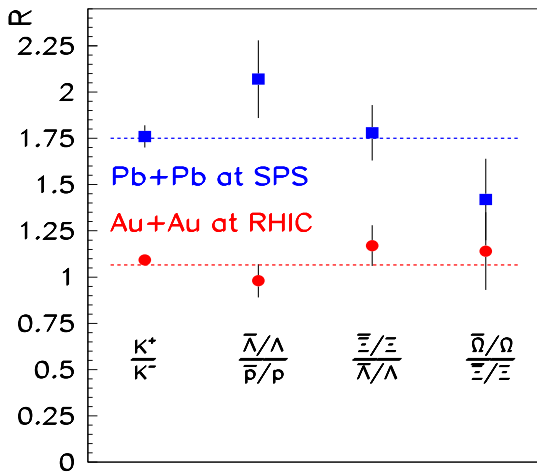


Figure 1. Graphical display of the particle ratios at mid-rapidity in Au+Au collision at RHIC [13] and in Pb+Pb collisions at SPS [17, 18, 19, 20].

4.3. Charge fluctuation in a quark-antiquark system

The charge fluctuation [21] is characterized by the ratio

$$D = 4 \frac{\langle \delta Q^2 \rangle}{\langle N_{ch} \rangle}, \quad (3)$$

where $\langle \delta Q^2 \rangle$ is the average of the charge fluctuation and $\langle N_{ch} \rangle$ is the average value of the charge multiplicity. The value of D is $D \approx 3$ for hadron gas in equilibrium, and $D \approx 1$ for the quark gluon plasma, The measured D value is near to 3. However, in the constituent quark coalescence scenario (ALCOR) one can also expect a $D \approx 3$ value.

4.4. Coalescence with constituent quark momentum conservation

The idea of quark coalescence can be applied at relatively large momenta and the hadron spectra at high- p_T can be investigated successfully [7, 8, 9]. In this kinematic region, especially at $p_T > 2$ GeV, the mass of the light and strange quarks can be neglected, $p_{quark} \gg m_{quark}$, and the calculations are simplified. Assuming that the most dominant kinematic window is overwhelming, then

$$p_a = p_b = P_h/2 \equiv P/2 \quad (4)$$

The expression for the meson emission spectrum [9]:

$$E \frac{dN_M}{d^3P} = \int_{\Sigma_f} d\sigma \frac{P \cdot u(r)}{(2\pi)^3} f_a(r; \frac{P}{2}) f_b(r; \frac{P}{2}). \quad (5)$$

A similar expression is valid for the baryon emission spectrum:

$$E \frac{dN_B}{d^3P} = \int_{\Sigma_f} d\sigma \frac{P \cdot u(r)}{(2\pi)^3} f_a(r; \frac{P}{3}) f_b(r; \frac{P}{3}) f_c(r; \frac{P}{3}). \quad (6)$$

These two equations lead to an interesting consequence: since the momentum distribution of constituent quarks is expected to behave as an exponentially decreasing function of transverse momentum, there are more partons at $P/3$ than at $P/2$.

$$f_q(r; \frac{P}{3}) > f_q(r; \frac{P}{2}) \quad (7)$$

From that follows, that we have more baryons than mesons in the momentum range where hadrons are produced by coalescence. This explains the surprising momentum dependence of the observed proton to meson ratio [7, 8, 9]. This description also implies the conservation of quark and antiquark numbers in the hadronization process.

4.5. The effective mass of quarks

Mass distribution of quarks

Since the effective mass of quarks are determined by their interaction with the neighborhood, and the matter in the fireball is not smooth and homogeneous, the granulated structure of the fireball is reflected in the effective mass distribution of the quarks.

The consequences of a possible quark mass distribution

$$\rho(m) = N e^{-\frac{\mu}{T_c}} \sqrt{\frac{\mu+m}{m+\mu}} \quad (8)$$

with $\mu = 0.25$ GeV and $T_c = 0.26$ GeV, are discussed in the next paragraph [10].

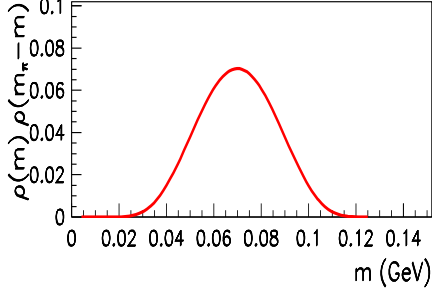


Figure 2. The product of the two quark mass distributions $\rho(m) \cdot \rho(m_\pi - m)$ in eq.(14). The maximum is at $m = m_\pi/2$.

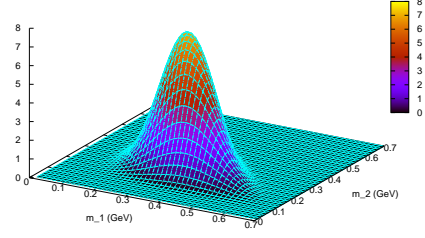


Figure 3. Product of three mass distributions in eq.(16). The horizontal axes are m_1 and m_2 , the mass m_3 is defined as $m_3 = m_B - (m_1 + m_2)$.

4.6. The coalescence expression for distributed quark mass

Using the covariant coalescence model of Dover *et al.*, [22], the spectra of hadrons formed from the coalescence of quark and antiquarks can be written as

$$E \cdot \frac{dN_h}{d^3\mathbf{p}} = \frac{dN_h}{dy\mathbf{p}_T d\mathbf{p}_T d\phi_p} = \frac{g_h}{(2\pi)^3} \int (p_h^\mu \cdot d\sigma_{h,\mu}) F_h(p_h; x_h). \quad (9)$$

Here $F_h(p_h; x_h)$ is an eight dimensional distribution (Wigner function) of the formed hadron, and $d\sigma$ denotes an infinitesimal element of the space-like hypersurface of hadron production.

Assuming that meson production is homogeneous within the reaction volume, the source function for the $a + b \rightarrow M$ meson production, $F_M(\mathbf{p}_M)$, is the following:

$$F_M(\mathbf{p}_M) = \int d^3\mathbf{p}_a d^3\mathbf{p}_b f_a(\mathbf{p}_a; 0) f_b(\mathbf{p}_b; 0) C_M(\mathbf{p}_a, \mathbf{p}_b, \mathbf{p}_M). \quad (10)$$

The coalescence function $C_M(\mathbf{p}_a, \mathbf{p}_b, \mathbf{p}_M)$ is defined as

$$C_M(\mathbf{p}_a, \mathbf{p}_b, \mathbf{p}_M) = \alpha_M \cdot e^{-((\mathbf{p}_a - \mathbf{p}_M/2)/P_c)^2} \cdot e^{-((\mathbf{p}_b - \mathbf{p}_M/2)/P_c)^2} \quad (11)$$

The parameters α_M and P_c reflect properties of the hadronic wave function in the momentum representation convoluted with the formation matrix element.

Assume that P_c is so small, that partons with practically zero relative momentum form a meson.

$$\mathbf{p}_a = \mathbf{p}_b = \mathbf{p}_M/2 \quad m_a + m_b = m_M \quad (12)$$

This leads to the meson coalescence function

$$C_M = \alpha_M \cdot \delta(\mathbf{p}_a - \mathbf{p}_M/2) \cdot \delta(\mathbf{p}_b - \mathbf{p}_M/2) \cdot \delta(m_a + m_b - m_M) \quad (13)$$

Thus we arrive at the following meson distribution function:

$$F_M(\mathbf{p}_t; 0) = \alpha_M \cdot \int_0^{m_M} dm_a \cdot \int_0^{m_M} dm_b \cdot \delta(m_M - (m_a + m_b)) \cdot \rho(m_a) \cdot f_q(\mathbf{p}_t/2; m_a) \cdot \rho(m_b) \cdot f_b(\mathbf{p}_t/2; m_b) \cdot \quad (14)$$

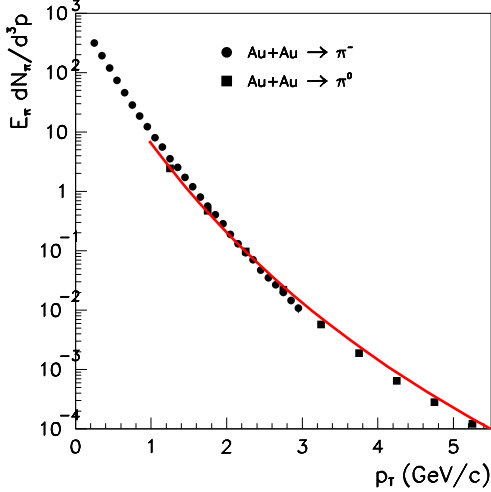


Figure 4. Measured [23] and calculated π^0 and π^- transvers momentum spectra in central Au+Au collisions at $\sqrt{s} = 200$ AGeV.

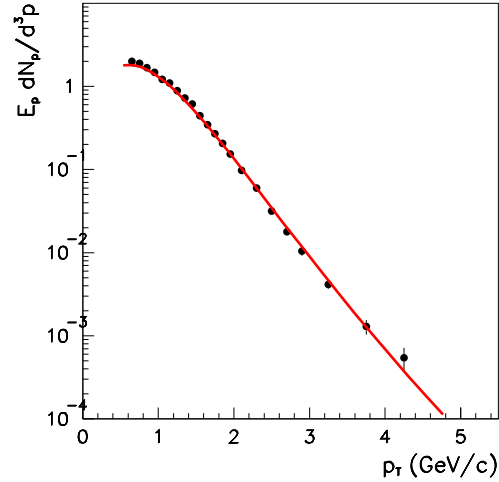


Figure 5. Measured [23] and calculated transverse momentum spectrum for antiproton production in central Au+Au collisions at $\sqrt{s} = 200$ AGeV.

Similar argumentation leads to the three-fold coalescence expression. In the place of eq.(12) we get:

$$\mathbf{p}_1 = \mathbf{p}_2 = \mathbf{p}_3 = \mathbf{p}_B/3 \quad m_1 + m_2 + m_3 = m_B \quad (15)$$

and the baryon source function becomes

$$F_B(\mathbf{p}_t) = \alpha_B \int_0^{m_{pr}} dm_1 \int_0^{m_{pr}} dm_2 \int_0^{m_{pr}} dm_3 \delta(m_B - (m_1 + m_2 + m_3)) \cdot \rho(m_1) f_q(\mathbf{p}_t/3, m_1) \cdot \rho(m_2) f_q(\mathbf{p}_t/3, m_2) \cdot \rho(m_3) f_q(\mathbf{p}_t/3, m_3) \cdot \quad (16)$$

The maximum contribution to the coalescence integral is obtained from the equal mass part of the mass distributions.

The calculated meson and baryon source functions and their space-time integrals in eq.(9) yield theoretical spectra comparable to experimental data [23]. In Figure 4 we display our results for pion production together with the experimental data on π^0 and π^+ production at mid-rapidity in Au+Au collisions at $\sqrt{s} = 200$ AGeV. Figure 5 shows calculation and data for antiproton. The agreement in the $0.5 < p_T < 5.0$ GeV momentum window is astonishing and proves the validity of the coalescence scenario.

Besides the hadron production on a logarithmic scale, we display the \bar{p}^-/π^- ratio in linear scale on Figure 6. The theoretical result is able to follow the tendencies of the anomalous antiproton to pion ratio.

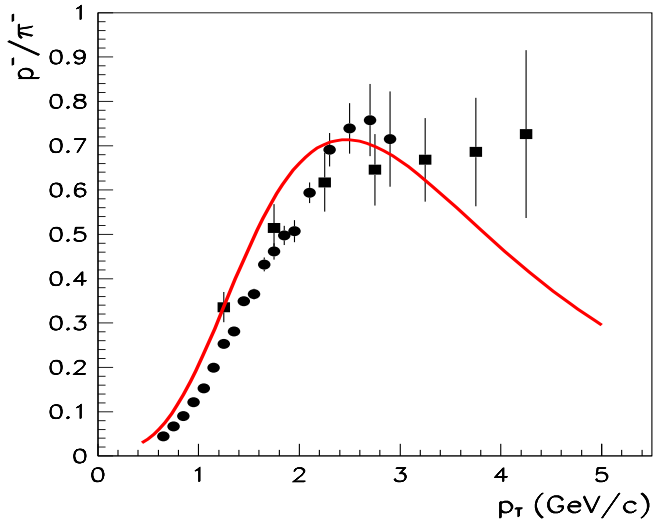


Figure 6. \bar{p}/π^- ratio as a function of p_T in central Au+Au collisions at $\sqrt{s} = 200$ AGeV. Experimental data points are from Ref. [23].

4.7. The v_2 paradox

The meson and baryon elliptic flow at high p_T show a peculiar behaviour, which is understandable in the framework of parton coalescence dynamics [24].

Assuming the following form for the asymmetric quark momentum distribution:

$$\frac{dN_q}{p_\perp dp_\perp d\Phi} = \frac{1}{2\pi} \frac{dN_q}{p_\perp dp_\perp} (1 + 2v_{2,q}(q_\perp) \cos(2\Phi)) \quad (17)$$

one gets in the coalescence dynamics for $v_2 \ll 1$ the hadron elliptic flow:

$$\begin{aligned} v_{2,M}(p_\perp) &\approx 2 * v_{2,q}(p_\perp/2) \\ v_{2,B}(p_\perp) &\approx 3 * v_{2,q}(p_\perp/3) \end{aligned} \quad (18)$$

This behaviour of the $v_{2,M}$ and $v_{2,B}$ parameters predicted by the coalescence hadronization dynamics are clearly observable in the experimental data (see Fig. 7).

The behaviour of flow asymmetry parameter

$$v_{2,u} = v_{2,d} = v_{2,s} \quad (19)$$

implies that the collective flow for quarks of all flavour is the same.

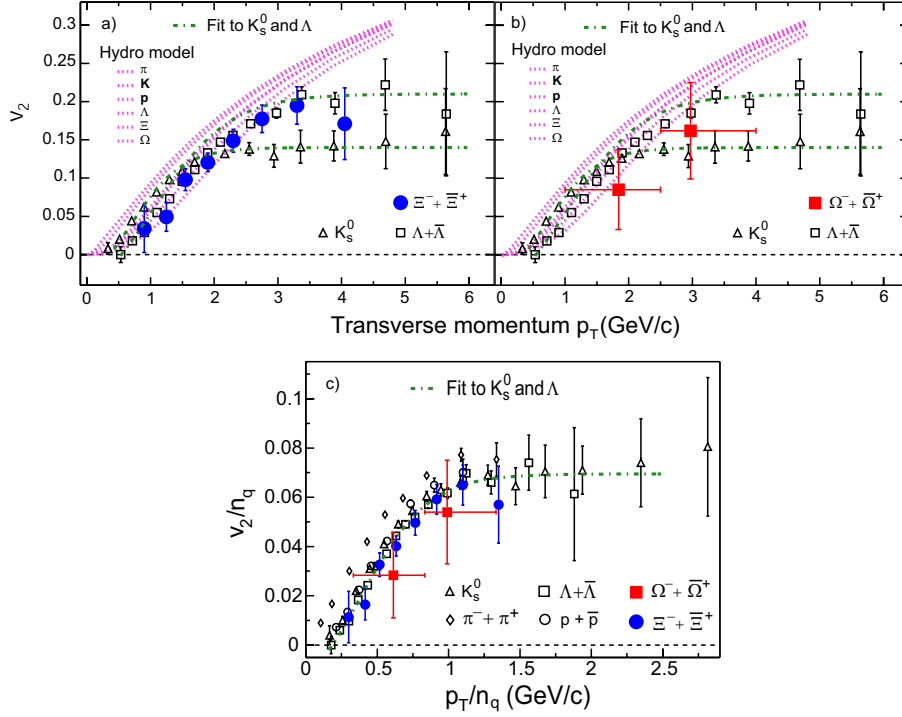


Figure 7. Measured baryon and meson elliptic flow (figure is from Ref. [25]).

5. Conclusion

A large number of experimental facts is in agreement with the assumption that *in the prehadronization stage*

- the quark matter consists of constituent quarks and antiquarks with effective mass;
- the collective flow for quarks of all flavor is the same;
- the hadronization proceeds via coalescence mechanism;
- the numbers of quarks and antiquarks are conserved during hadronization.

Further

- the initial stage of heavy ion collision is strong color field (gluon) dominated;
- the final stage of heavy ion collision is quark dominated.

REFERENCES

1. B. Müller, *The Physics of quark - gluon plasma*, Lecture Notes in Physics, vol. 225, Springer, 1985, and references therein. T.S. Biró and J. Zimányi, Phys. Lett. **B113** (1982) 6; J. Rafelski and B. Müller, Phys. Rev. Lett. **48** (1982) 1066; T.S. Biró and J. Zimányi, Nucl. Phys. **A395** (1983) 525.
2. M. Gyulassy and L. McLerran, Nucl. Phys. **A750** (2005) 30.
3. M. Gyulassy, P. Lévai, and I. Vitev, Phys. Rev. Lett. **85** (2000) 5535; Nucl. Phys. **B594** (2001) 371.
4. P. Lévai and U. Heinz, Phys. Rev. **C57** (1998) 1879.
5. T.S. Biró, P. Lévai, and J. Zimányi, Phys. Lett. **B347** (1995) 6; J. Phys. **G27** (2001) 439; J. Phys. **G28** (2002) 1561.
6. A. Bialas, Phys. Lett. **B442** (1998) 449; J. Zimányi, T.S. Biró, T. Csörgö, P. Lévai, Phys. Lett. **B472** (2000) 243.
7. R.C. Hwa and C.B. Yang, Phys. Rev. **C66** (2002) 025205; Phys. Rev. Lett. **90** (2003) 212301; Phys. Rev. **C70** (2004) 024905.
8. V. Greco, C.M. Ko, and P. Lévai, Phys. Rev. Lett. **90** (2003) 202302; Phys. Rev. **C68** (2003) 034904.
9. J. Fries, S.A. Bass, B. Müller, and C. Nonaka, Phys. Rev. Lett. **90** (2003) 202303; Phys. Rev. **C68** (2003) 044902.
10. J. Zimányi, T.S. Biró, and P. Lévai, J. Phys. **G31** (2005) 711.
11. C. Adler *et al.*, (STAR Collaboration), Phys. Rev. Lett. **87** (2001) 112303.
12. C. Adler *et al.*, (STAR Collaboration), Phys. Lett. **B595** (2004) 143.
13. J. Adams *et al.*, (STAR collaboration), Phys. Lett. **B567** (2003) 167.
14. C. Adler *et al.*, STAR collaboration), Phys. Rev. Lett. **86** (2001) 4778; *Erratum-ibid.* **90** (2003) 119903(E).
15. J. Adams *et al.*, (STAR collaboration), Phys. Rev. Lett. **92** (2004) 182301.
16. P. Fachini *et al.*, (STAR Collaboration), J. Phys. **G28** (2002) 1599.
17. S.V. Afanasiev *et al.*, (NA49 Collaboration), Nucl. Phys. **A715** (2003) 161.
18. S.V. Afanasiev *et al.*, (NA49 Collaboration), Phys. Rev. **C66** (2002) 054902.
19. S.V. Afanasiev *et al.*, (NA49 Collaboration), Nucl. Phys. **A715** (2003) 453.
20. S.V. Afanasiev *et al.*, (NA49 Collaboration), Phys. Lett. **B538** (2003) 275.
21. A. Bialas, Phys. Lett. **B532** (2002) 249.
22. C. Dover, U. Heinz, E. Schnedermann, and J. Zimányi, Phys. Rev. **C44** (1991) 1636.
23. S.S. Adler *et al.*, (PHENIX Collaboration), Phys. Rev. **C69** (2004) 034909.
24. D. Molnár and S.A. Voloshin, Phys. Rev. Lett. **91** (2003) 092301.
25. J. Adams *et al.*, (STAR Collaboration), Phys. Rev. Lett. **95** (2005) 122301.